Journal of Magnetic Resonance 242 (2014) 33–40

Contents lists available at ScienceDirect

Journal of Magnetic Resonance

journal homepage: www.elsevier.com/locate/jmr

# Straightforward measurement of individual $^1J(CH)$ and $^2J(HH)$ in diastereotopic $CH_2$ groups

Josep Saurí, Laura Castañar, Pau Nolis, Albert Virgili, Teodor Parella *

*Servei de Ressonància Magnètica Nuclear and Departament de Química, Universitat Autònoma de Barcelona, E-08193 Bellaterra, Catalonia, Spain*

ARTICLE INFO

*Article history:*
Received 17 December 2013
Revised 31 January 2014
Available online 12 February 2014

*Keywords:*
E.COSY
One-bond proton–carbon coupling constants
Two-bond proton–proton coupling constants
Methylene spin systems
Inverse INEPT
Residual dipolar couplings

ABSTRACT

The C–$H_A$ cross-peak corresponding to a diastereotopic $CH_AH_B$ methylene spin system exhibits a characteristic 1:0:1 multiplet pattern along the indirect dimension of a $\omega_1$-coupled HSQC spectrum. It is shown here that the use of the initial $^{13}C$ Boltzmann polarization instead of the regular INEPT-based $^1H$ Boltzmann polarization makes visible the central lines of this multiplet pattern. A spin-state-selective method is proposed for the efficient measurement of both $^1J(CH_A)$ and $^1J(CH_B)$ along the indirect dimension of a 2D spectrum as well as to the magnitude and the sign of the geminal $^2J(H_AH_B)$ coupling constant from the straightforward analysis of a single four-component E.COSY cross-peak. Additionally, the extraction of $^1J(CH)$ values for CH and $CH_3$ multiplicities can be also performed from the same spectrum. The success of the method is also illustrated for the determination of residual dipolar $^1D(CH)$ and $^2D(HH)$ coupling constants in a small molecule weakly aligned in a PMMA swollen gel.



## 1. Introduction

In recent years, it has appeared an enormous interest for the measurement of scalar and residual dipolar (RDC) one-bond proton–carbon coupling constants ($^1J(CH)$ and $^1D(CH)$, respectively) in small molecules dissolved in weakly aligned anisotropic media [1–3]. HSQC-based pulse schemes have been generally chosen for this purpose and the accuracy and the simplicity on the experimental measurement of $^1J(CH)$ are subjects of discussion. Some topics of recent interest have been (i) the design of general and robust NMR methods that works efficiently for all multiplicities, (ii) the discussion about whether the $^1J(CH)$ splitting should be measured from the direct $\omega_2$ ($^1H$) or the indirect $\omega_1$ ($^{13}C$) dimension, (iii) the accurate measurement of $^1J(CH)$ for individual protons in diastereotopic $CH_2$ or $NH_2$ groups, or (iv) the simultaneous determination of additional coupling constants from the analysis of the same cross-peak, being the maximum interest the sign-sensitive determination of geminal $^2J(HH)$ values.

The measurement of $^1J(CH)$ from the detected dimension is relatively easy and high levels of digital resolution are readily available. For instance, the CLIP-HSQC experiment prove to be an efficient tool to determine the $^1J(CH)$ value from the resulting clean in-phase doublets [4]. However, strong J(HH) coupling effects can generate a high degree of asymmetry between the high- and low-field multiplet lines in $\omega_2$-coupled HSQC spectra, which can preclude reliable determination of $^1J(CH)$ coupling constants values. In addition, broad signals and/or the large contributions of RDCs can generate poorly defined multiplets that make difficult accurate measurements. These drawbacks have already been described, particularly for CH spin systems in carbohydrates or on the typical strong geminal interaction found in diastereotopic $CH_2$ spin systems, and some practical solutions have been proposed [5–9]. To avoid such inconveniences, the measurement of $^1J(CH)$ along the $\omega_1$ dimension have been advisable [9,10] although this requires the need for a large number of $t_1$ increments, and therefore longer acquisition times. The successful use of non-linear uniform sampling, J scaling factors or spectral folding can speed up data acquisition and/or increase the digital resolution in the $\omega_1$ dimension [10].

The accurate measurement of $^1J(CH)$ for individual protons in diastereotopic $CH_AH_B$ (or $NH_AH_B$) groups is one of the most challenging tasks in this field. Several methods have been proposed that measure them from the $\omega_1$ or $\omega_2$ dimension, but they all present some drawback that can prevent their general use [11–25]. For instance, the passive $^1J(C–H_B)$ value can be separately measured into the active $H_A$ cross-peak, and vice versa, along the $\omega_1$ dimension of a J-resolved HMQC experiment [11]. In addition, the large doublet is further split by the $^2J(H_AH_B)$ coupling yielding a double-doublet. The disadvantage is that additional experiments can

* Corresponding author.
*E-mail address:* teodor.parella@uab.cat (T. Parella).

http://dx.doi.org/10.1016/j.jmr.2014.02.003
1090-7807/

be needed to measure $^1$J(CH) for CH or $CH_3$ spin systems. $^{13}$C-edited versions of the 2D $^1$H J-resolved experiment have been proposed to resolve enantiomeric derivatives dissolved in anisotropic media by visualizing their different $^1$J(CH) splitting sizes along the indirect dimension [12,13]. Other related J-resolved HSQC experiments have been also described but they can require time-consuming 3D data acquisition [14] or the collection of multiple 2D J-modulated data [15,16]. An important group of NMR experiments are those based on spin-state selection specifically designed for methylene groups [8,17–25]. Some reported examples should be the P.E.HSQC [8] SPITZE [17] or $CH_2$-TROSY [19,20] experiments that yield simplified coupling patterns, and where the sign and the magnitude of the geminal $^2$J(HH) can be additionally extracted. In all these cases, the central lines of the $\omega_1$-multiplet corresponding to a $CH_2$ group are not observed, and therefore only the sum of the two $^1$J(CH) can be determined from the indirect dimension.

In the present study, a new 2D $\omega_1$-coupled inverse INEPT experiment (referred to as $\omega_1$-iINEPT) is proposed for the observation of the missing central lines in diastereotopic $CH_2$ cross-peaks. The resulting cross-peak present a characteristic E.COSY multiplet pattern that facilitates the straightforward measurement of both individual $^1$J($CH_A$) and $^1$J($CH_B$) values, as well as the sign and magnitude of the geminal $^2$J(HH) coupling. The method starts exclusively from $^{13}$C Boltzmann polarization, it is driven with broadband $^{13}$C decoupling during $^1$H acquisition and, very importantly, also works for CH and $CH_3$ multiplicities. The experiment is easily adapted for a J-resolved presentation (referred to as $\omega_1$-iINEPT-J) which allows obtain higher levels of resolution within the same experimental time by the use of a reduced spectral width in the indirect dimension [11–13,26,27]. The success of the method is illustrated for several samples and particular cases and as well as for the measurement of small residual coupling constants in small molecules dissolved in a weakly aligned media.

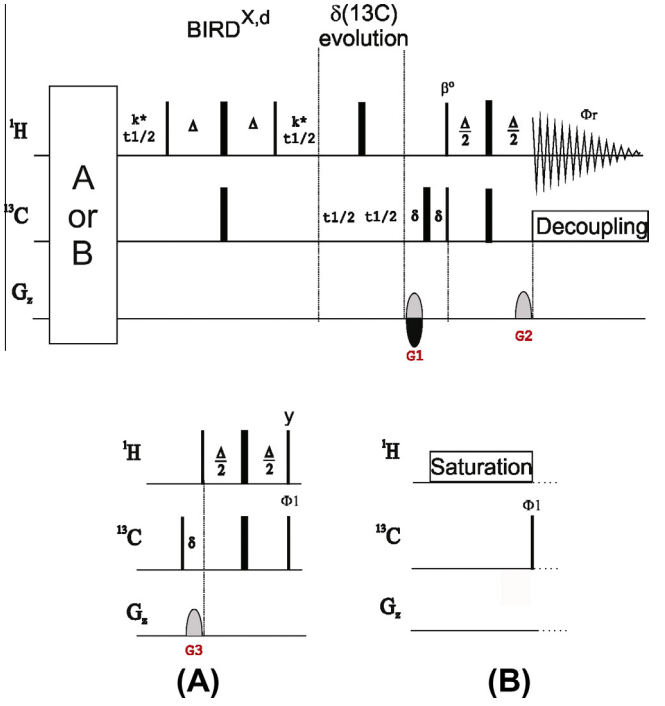


**Fig. 1.** Pulse sequences for the (A) $\omega_1$-HSQC and (B) $\omega_1$-iINEPT experiments. Thin and thick rectangles represent 90° and 180° rectangular pulses, respectively, applied along the *x* axis unless indicated differently. A basic two-step phase cycling is applied: $\varphi_1 = x,-x$; $\varphi_{rec} = x,-x$. A small flip angle ($\beta = 36°$) generates E.COSY cross-peaks. Inversion and refocusing 180° $^{13}$C pulses can be applied as adiabatic pulses and the element labeled as $\delta(^{13}C)$ evolution period is optional. The inter-pulse delays in INEPT and BIRD elements are optimized according to $\Delta = 1/(2 * {}^1J(CH))$. The echo/anti-echo encoding of $\omega_1$ frequencies was achieved by changing the sign of G1 between successive $t_1$ increments. The ratio between G1:G2:G3 were 80:20.1:13. The duration of a pulse-field gradient (PFG) and of the subsequent recovery delay amounts to $\delta$.

## 2. Results and discussion

The idea to develop the $\omega_1$-iINEPT experiment was born from the recent P.E.HSQMBC experiment, which was devised to measure three different $^1$J(CH), $^2$J(HH) and a $^n$J(CH) coupling constants from a single 2D cross-peak [28]. Other related works that have inspired us were the P.E.HSQC [8] and the BIRD-HSQC [9] experiments, this latter being further refined and evaluated by Thiele and Bermel (see Fig. 1c in Ref. [10]). The basic pulse scheme of the reference $\omega_1$-coupled HSQC ($\omega_1$-HSQC) experiment uses the traditional $^1$H Boltzmann polarization as a starting point (Fig. 1A). In the following, we consider an isolated diastereotopic $CH_AH_B$ spin system defined with three different $^1$J($CH_A$), $^1$J($CH_B$) and $^2$J($H_AH_B$) coupling constants. The sequence starts with an initial 90° ($^{13}$C)-gradient element to remove any contribution coming from the $^{13}$C Boltzmann polarization. After the $^1$H-to-$^{13}$C INEPT transfer, anti-phase $^{13}$C magnetization is present as a mixture of $2H_{Az}C_y + 2H_{Bz}C_y$, which evolve under the effects of $^1$J(CH) and $\delta(^{13}C)$ in a sequential mode, by using separated and synchronously incremented time periods. Thus, the magnetization evolves first under the effect of a BIRD$^{d,X}$ element [29,30] flanked by a variable J-scaled $t_1$ evolution period (defined by a scaling factor $k$) to allow the exclusive evolution of $^1$J(CH) whereas $^{13}$C chemical shift and long-range CH contributions are refocused, and then $^{13}$C chemical shift can evolve from an optional $t_1$ evolution period as usual. In the subsequent analysis, the scaling factor, which is set arbitrarily within the limits set by relaxation and/or signal overlapping, the effects of the labeling G1 gradient and the optional $^{13}$C chemical shift $t_1$ evolution period are neglected for the sake of clarity. Thus, for a single $H_A$ spin, the evolution during the variable $t_1$ BIRD-based period ($k = 1$) is described as:

$$2H_{Az}C_y[\cos(\pi^1J(CH_A)t_1)\cos(\pi^1J(CH_B)t_1) - \sin(\pi^1J(CH_A)t_1) \times \sin(\pi^1J(CH_B)t_1)] \quad (1)$$

Applying the trigonometric relationship $\cos A\cos B - \sin A\sin B = \cos(A + B)$, we obtain

$$2H_{Az}C_y\cos(\pi^1J(CH_A + {}^1J(CH_B))t_1) \quad (2)$$

meaning that only the outer lines of the theoretical triplet or double-doublet coupling pattern of the methylene proton cross-peak would be observed and, therefore, only the sum of the both couplings ($^1$J($CH_A$ + $^1$J($CH_B$)) will be observed as an in-phase doublet along the indirect dimension (Fig. 2A) [15]. This dependence with respect to the cosine function makes that multiplet patterns with relative intensities of 1:1 for CH, 1:0:1 for $CH_2$, and 3:1:1:3 for $CH_3$ will be displayed along the $\omega_1$ dimension [8,34]. A key feature introduced in the last refocusing INEPT block is the small-flip $^1$H pulse angle ($\beta = 36°$) which generates simplified E.COSY multiplet patterns for non-equivalent protons in $CH_2$ and $CH_3$ spin systems (Fig. 2B) [8,31–33].

To improve the appearance and usefulness of cross-peaks obtained from $\omega_1$-iINEPT experiments, we propose to start the experiment with the initial $^{13}$C Boltzmann polarization instead of the INEPT-based $^1$H Boltzmann polarization because this leads to interesting changes in the central lines of methylene cross-peaks, as known for the analogous old $^{13}$C-detected heteronuclear J-resolved 2D experiment [35]. The initial 90° $^{13}$C pulse, applied after an

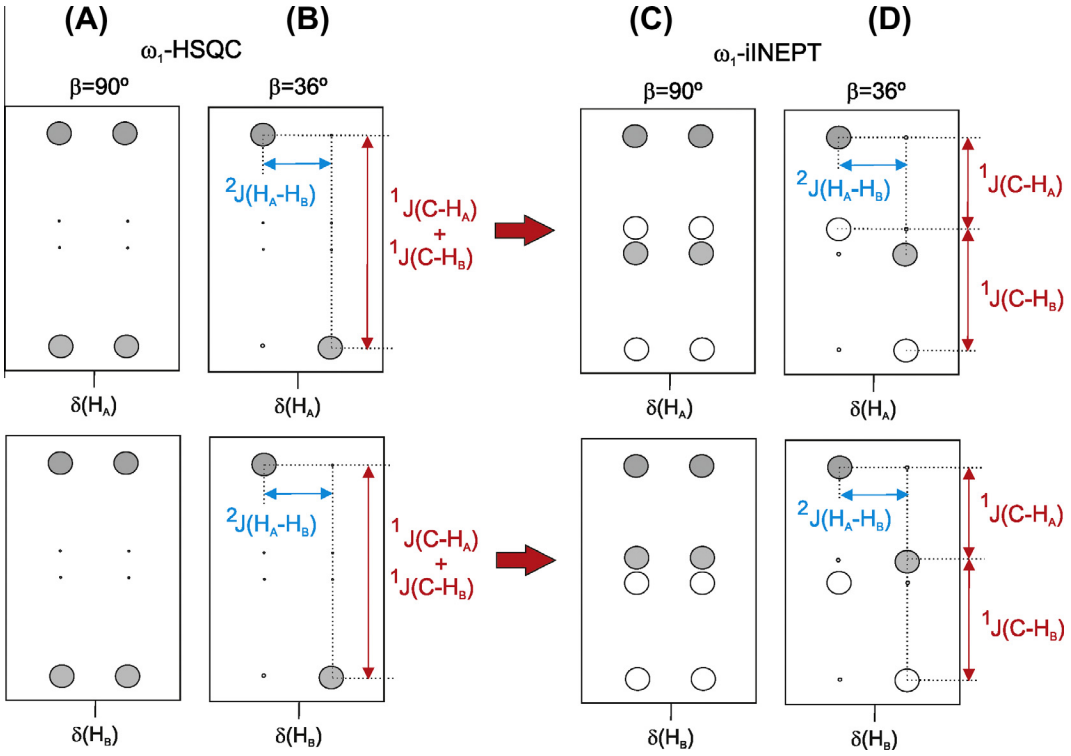


**Fig. 2.** Schematic representation of the 2D multiplet pattern of each individual $H_A$ and $H_B$ proton belonging to a methylene $CH_AH_B$ group. (A and B) $^1$H-Boltzmann polarization driven ($\omega_1$-HSQC) experiments using $\beta = 90°$ and 36°, respectively, and (C and D) $^{13}$C-Boltzmann polarization driven experiments ($\omega_1$-iINEPT) using $\beta = 90°$ and 36°, respectively. In (D), the magnitude and the sign of all involved couplings (defined as $^2J(H_AH_B)$ and assuming $^1J(CH_A) < {}^1J(CH_B)$) can be readily extracted. Open and dotted circles represent peaks with opposite phase.

heteronuclear NOE enhanced pre-scan period by means of a $^1$H WALTZ-16 pulse train saturation, generates in-phase $-C_y$ magnetization (Fig. 1B) which evolves under the effect of $^1J$(CH) during the variable $t_1$ BIRD-based period:

$$-2H_{Az}C_x[\sin(\pi^1J(CH_A)t_1)\cos(\pi^1J(CH_B)t_1)] - 2H_{Bz}C_x[\cos(\pi^1J(CH_A)t_1)\sin(\pi^1J(CH_B)t_1)] \quad (3)$$

The result is a pure absorptive 2D $\omega_1$-iINEPT spectra displaying double-doublet coupling patterns along the $\omega_1$ dimension for each individual $H_A$ or $H_B$ cross-peaks, that initially would consist of eight different components as shown in Fig. 2C. Analyzing only the $H_A$ spin, it will show an anti-phase doublet pattern with respect to $^1J(CH_A)$ (sine modulated) and an additional in-phase doublet pattern with respect to $^1J(CH_B)$ (cosine modulated) along the $\omega_1$ dimension. As discussed before, the effect to apply a small flip angle ($\beta = 36°$) will generate a simplified four-component cross-peak with a characteristic E.COSY multiplet pattern due to the mutual $^2J(H_AH_B)$ (Fig. 2D), which facilites both the multiplet interpretation and analysis (see Fig. S1; supporting information). Thus, the active $^1J(CH_A)$ coupling is directly extracted from the anti-phase 1:−1 pattern along the same column in $\omega_1$, whereas the passive $^1J(CH_B)$ coupling can be also extracted directly by measuring the in-phase components in each part of the E.COSY pattern. Otherwhise, the sign and the magnitude of $^2J$(HH) is easily extracted from the frequency separation between tilted peaks along the w2 dimension. Fig. 2 summarizes the expected cross-peak pattern for a single diastereotopic $CH_AH_B$ proton using the different $\omega_1$-HSQC and $\omega_1$-iINEPT approaches with $\beta = 90°$ and 36°. For CH groups, a doublet with relative 1:−1 intensities is obtained whereas a 1:1:−1:−1 coupling pattern will be displayed for a $CH_3$ group.

As a first example, Fig. 3A and B shows the equivalent $\omega_1$-HSQC and $\omega_1$-iINEPT correlation spectra, respectively, of strychnine (**1** in Scheme 1) acquired with the pulse schemes of Fig. 1, under the same experimental conditions and using a scaling factor of $k = 8$. The general coupling pattern for individual CH and $CH_2$ groups are marked with highlighted boxes. CH cross-peaks present the same doublet structure in both approaches. On the other hand, whereas the central lines for each individual $CH_2$ cross-peak are absent in the $\omega_1$-HSQC spectrum, they are clearly distinguished in the $\omega_1$-iINEPT version. A close inspection of the multiplet patterns for $CH_2$ cross-peaks in both spectra reveals the simplified E.COSY multiplet structure as described in other related experiments [8,19]. Also note the different in-phase *vs* anti-phase pattern behavior along the indirect dimension, although this is not relevant for the measurement. In cases where chemical shift assignment is already known and/or signal overlapping is not severe, the proposed method can be recorded in a J-resolved mode by simple omission of the $^{13}$C chemical shift evolution period ($t_{1/2} - 180°(^1H) - t_{1/2}$). In this way the spectral width in the indirect dimension could be reduced by a factor of about 40, from 20,000 Hz (160 ppm at 500 MHz) to 500 Hz, and therefore the spectral resolution in $\omega_1$ should be improved by a similar factor if all other experimental conditions remain the same. Fig. 3C and D shows the equivalent $\omega_1$-HSQC-J and $\omega_1$-iINEPT-J spectra, respectively, acquired with the same number of $t_1$ increments and using an scaling factor of $k = 1$. It can be observed that the absence of $^{13}$C chemical shift signal dispersion does not introduce a serious problem on severe signal overlapping in a small molecule like **1**, where all cross-peaks can be succesfully analyzed. All the discussion and conclusions described in Ref. [10] about the application of non-linear sampling to accelerate data acquisition and/or to increase digital resolution in the indirect dimension could

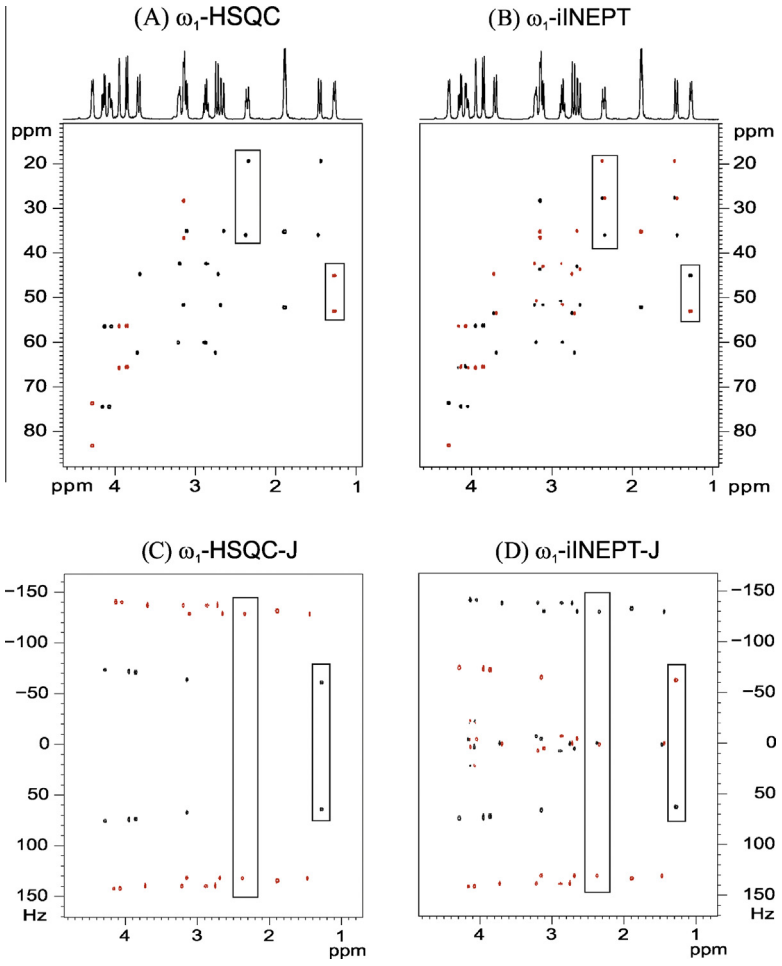


**Fig. 3.** 2D $^{1}H–^{13}C$ spectra of **1** acquired with the pulse sequences of Fig. 1. (A) $\omega_1$-HSQC and (C) $\omega_1$-HSQC-J spectra were obtained starting from $^{1}H$ Boltzmann magnetization, and (B) $\omega_1$-iINEPT and (D) $\omega_1$-iINEPT-J spectra were achieved starting from $^{13}C$ Boltzmann magnetization. (A) and (B) are heteronuclear correlation maps (acquired with an scaling factor of $k = 8$) whereas (C) and (D) are the corresponding J-resolved versions (scaling factor $k = 1$ and omission of the $^{13}C$ chemical shift $t_1$ evolution period). All spectra were acquired and processed under the same experimental conditions. 2 scans were collected for each one of the 256 $t_1$ increments using a pre-scan delay of 3 s. Squared boxes mark specific CH and diastereotopic $CH_2$ cross-peak as examples in each spectrum.

be extrapolated here for the proposed methods. Further increase of resolution by a factor of 3 can be additionally achieved by allowing signal folding in the indirect dimension (see Fig. S2 in the supporting information for an example provided using a reduced spectral width of 180 Hz).

Fig. 4 shows an expanded area of the 2D $\omega_1$-iINEPT-J spectrum, where the clean tilt, the straightforward analysis and the excellent resolution of the resulting peak patterns can be quickly observed. Note the perfect equivalence between the cross peaks of diastereotopic protons (for instance H-18a *vs* H-18b or H-11a *vs* H-11b) which permit the easy and direct measurement of the same three different involved couplings ($^{1}J(CH_A)$ and $^{1}J(CH_B)$ as well as the geminal $^{2}J(HH)$) from two independent cross-peaks. The comparison of the experimental J values extracted from these two different measurements evaluates the accuracy of the measurement, and also ensures the measurement of all couplings even in the case of accidental signal overlapping of one of the two diastereotopic proton prevents its analysis. For well resolved $^{2}J(HH)$ values, the difference between diastereotopic $^{1}J(CH)$ values is quickly ascertained from the relative displacement between the two central lines and accurate $^{1}J(CH)$ values can be easily measured even in the case of minor differences between $^{1}J(CH_A)$ and $^{1}J(CH_B)$. For instance, whereas a small difference smaller than 2 Hz is measured for the H-15a/H-15b pair, a big difference about 14.5 Hz is found for H-18a/H-18b. Experimental $^{1}J(CH)$ and $^{2}J(HH)$ data extracted from these spectra for compound **1** are in agreement with those reported previously in other works (see Table S1 in the supporting information) [5,36–39]. Even in the case of signal overlapping, CH cross-peaks can be easily distinguished from those of $CH_2$ groups by their different doublet or double-doublet coupling patterns and also from the relative opposite phase of the anti-phase components for $CH/CH_3$ and $CH_2$ groups because the BIRD element acts as a multiplicity-editing element. For instance, note the clear distinction and straightforward measurement that can be performed for the three different protons resonating close to 3.1–3.2 ppm.

When two diastereotopic protons have similar chemical shift and $^{1}J(CH)$ values, the central lines can be partially or completely cancelled, as shown for the H-17a/H-17b protons resonating at 1.9 ppm in Fig. 3D. Another special case is when the geminal $^{2}J(HH)$ is near to 0 Hz, where the distinction of the four E.COSY components will depend of the different $^{1}J(CH)$ sizes. One illustrative example is the H-8a and H-8b olefinic protons belonging to the exocyclic $CH_2$ group in 5-methylene-2-norbornene (**2**) (Fig. 5A) which present unresolved signals in the conventional $^{1}H$ spectrum, and where the mutual $^{2}J(H8a–H8b)$ coupling can not be directly measured. The well differentiated four components observed in the $\omega_1$-iINEPT-J spectra allow a measurement of $^{2}J(HH) = +1.1$ Hz,

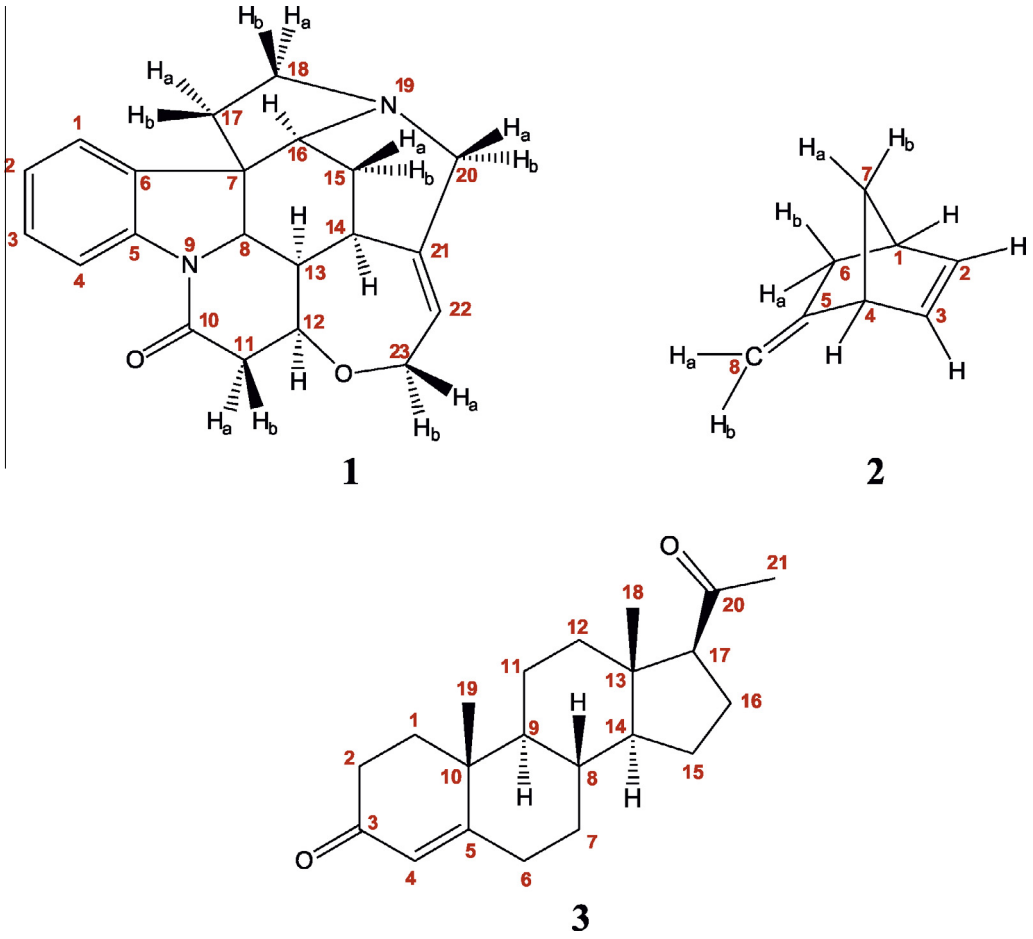


**Scheme 1.** Molecules used in this work.

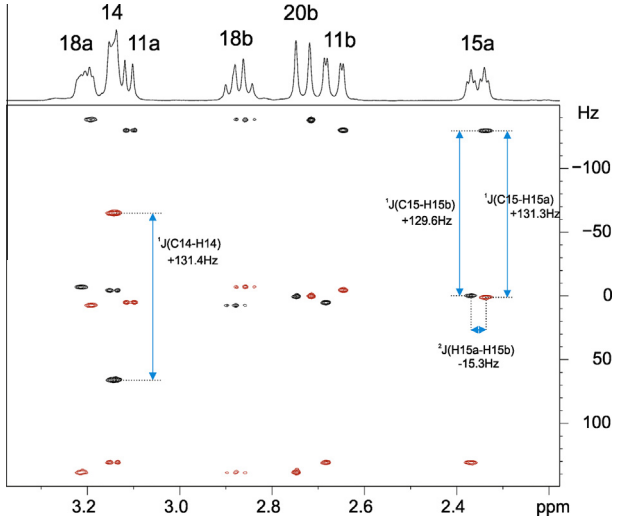


**Fig. 4.** Expanded area corresponding to the $\omega_1$-iINEPT-J spectrum of Fig. 3D, where the different multiplet patterns for a CH group and several diastereotopic $CH_2$ spin systems can be clearly visualized and analyzed, and all $^1J(CH)$ and $^2J(HH)$ can be measured with simplicity and accuracy.

where the positive sign can be determined by comparison with the opposite E.COSY tilt presented by other diastereotopic H-6 and H-7 methylene protons, which have large negative $^2J(HH)$ values of −15.3 Hz and −8.1 Hz, respectively. Although there are small differences between the two central lines, the measurement of each individual $^1J(CH)$ (155.1 *vs* 157.1 Hz) can be performed twice, independently from each cross-peak and with a minimal deviation of ±0.1 Hz (Table S2; supporting information).

The simplicity of the proposed $\omega_1$-iINEPT methods make them highly interesting for the measurement of small $^1D(CH)$ and $^2D(HH)$ RDCs, by comparison the difference between experimental measurements performed in isotropic *vs* anisotropic conditions ($D = T_{(aniso)} - J_{(is)}$). Compound **2** was weakly aligned in a poly(-methyl methacrylate) (PMMA) gel swollen in $CDCl_3$ using the reversible compression/relaxation method [40] , and $^1D(CH)$ and $^2D(HH)$ RDCs magnitudes and signs could be easily determined for all signals (see Fig. S3C; supporting information). Fig. 5 compares some cross-peaks obtained in both isotropic and anisotropic conditions. It can be seen how the relative orientation of each diastereotopic HH pair is clearly differentiated from their $^2D(HH)$ values: −0.2 Hz for H-8a/H-8b protons, −4.1 Hz for H-6a/H-6b protons and +3.1 Hz for H-7a/H-7b protons. A list of all measured scalar and residual dipolar coupling constants can be found in Table S2 of the supporting information.

The last example corresponds to a molecule having a more complex $^1H$ spectrum, progesterone (**3**), with high levels of signal overlapping in its aliphatic region. Fig. 6 shows an expanded area of the $\omega_1$-iINEPT spectrum, where cross-peaks for all multiplicites can be distinguished and the corresponding $^1J(CH)$ and $^2J(HH)$ values conveniently measured (see Table S3 in the supporting information). For instance, note the excellent signal dispersion and multiplet editing for the five resonances fully overlapped in the 1.5–1.65 ppm area. Accidental overlapping of multiplet components

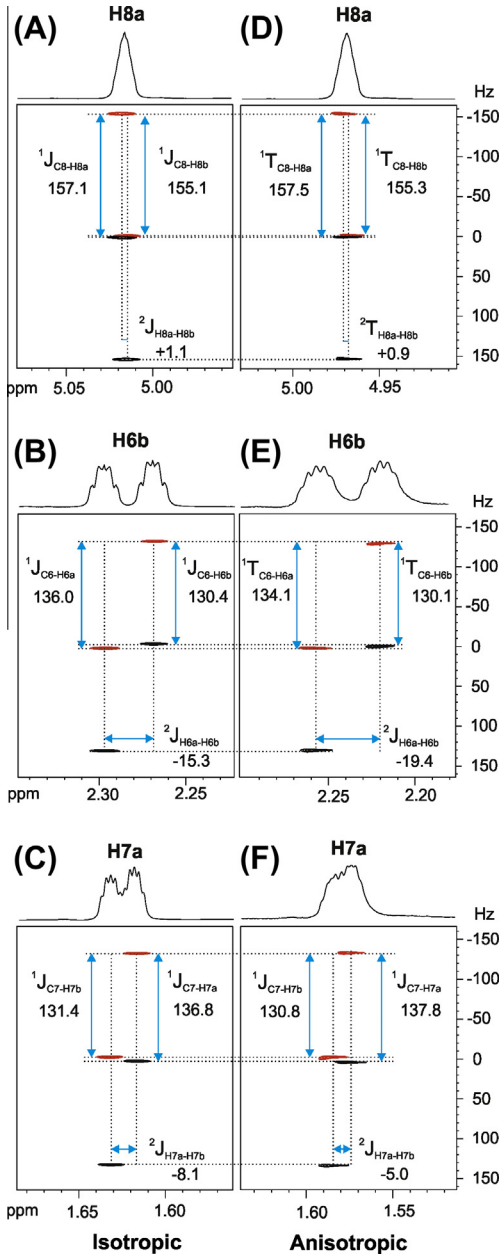


**Fig. 5.** Some illustrative 2D cross-peaks extracted from the $\omega_1$-iINEPT-J spectra of **2** showing the easy measurement of the experimental $^1J(CH)/^1T(CH)$ and $^2J(HH)/^2T(HH)$ values measured in (A–C) isotropic ($CDCl_3$) and (D–F) anisotropic (weakly aligned in PMMA gel swollen in $CDCl_3$) conditions. Similar values for the same couplings are also measured from the cross-peaks of the other diastereotopic protons (see a complete set of coupling values in Table S2 in the Supporting information).

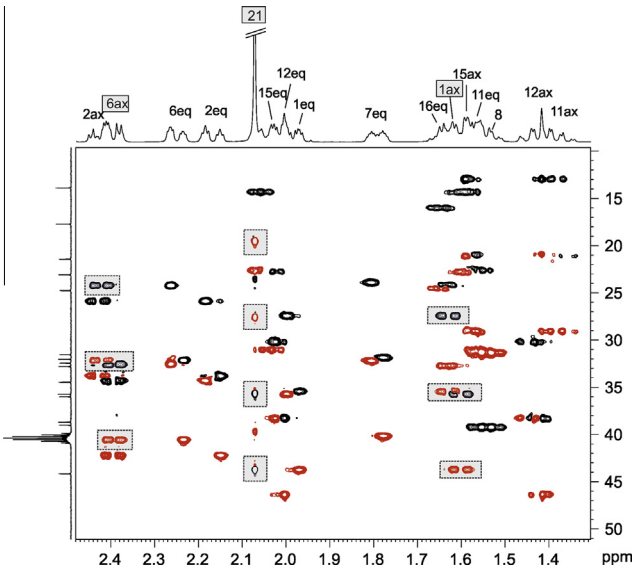


**Fig. 6.** Expanded area of the 2D $\omega_1$-iINEPT spectrum of **3** acquired with 4 scans for each one of the 256 $t_1$ increments, and using a pre-scan delay of 3 s. Boxes enhance the different components corresponding to the H-6ax and H-1ax protons. In addition, the 1:1:−1:−1 multiplet corresponding to the methyl group 21 (at 2.08 ppm) is also highlighted.

can be overcomed by using the J-resolved version or by changing the scaling factor. The diastereotopicity in the three protons belonging to a methyl groups is not observed and they usually appear as a singlet due to their free rotation under isotropic conditions. However, in analogy with the discussion presented here for diastereotopic $CH_2$ spin systems, the same conclusions could be extracted from the analysis of a hypothetical non-equivalent protons in a $CH_3$ group [8,41]. Whereas isotropic $CH_3$ cross-peaks with no distinction between equivalent protons present a typical 3:1:1:3 multiplet pattern in $\omega_1$-HSQC experiments [34], they display a symmetrical 1:1:−1:−1 coupling pattern in the $\omega_1$-iINEPT, as seen for the Me-21 in Fig. 6. A modified HSQC experiment has been reported to recover the 1:2:1 and 1:3:3:1 pattern in $NH_2$ and $NH_3^+$ groups, respectively, and spin-state selected methods to study analysis have been used to study differential relaxation of the different line multiplets of methyl cross-peaks in proteins [41].

In terms of sensitivity, the $\omega_1$-iINEPT experiment present a sensitivity decrease when compared to the analog $\omega_1$-HSQC experiment, because of the differential signal enhancement achieved by heteronuclear polarization transfer via INEPT or by heteronuclear NOE effects. In addition, the pre-scan delay must be optimized as a function to the longer $^{13}C$ $T_1$ values, although that protonated carbons relax relatively fast. Our experimental data confirms such theoretical prediction and signal-to-noise enhancements by a factor of about 3 and 4 can be achieved for $\omega_1$-iINEPT and $\omega_1$-HSQC experiments, respectively, when compared with a reference non signal-enhanced $\omega_1$-iINEPT experiment acquired without proton saturation and a pre-scan delay of 3 s (see Fig. S4 in the supporting information). Although the proposed methodology could distinguish diastereotopic protons in $NH_2$ groups, the large difference in sensitivity enhancement achieved by polarization transfer when compared with those obtained by direct $^{15}N$ Boltzmann magnetization without NOE enhancement (a theoretical factor about 10) makes the experiment of limited practical use due to its very low sensitivity. In addition, the two central lines are likely to be quite broad for large molecules.

In summary, a general and simple NMR method to obtain a characteristic spin-state-selected multiplet pattern for diastereotopic $CH_AH_B$ methylene systems has been described. The magnitude and the sign of the three involved coupling values ($^1J(CH_A)$, $^1J(CH_B)$ and $^2J(H_AH_B)$) can be measured simultaneously from the analysis of a single and clean four-component E.COSY cross-peak. The method also measures $^1J(CH)$ for all other carbon multiplicities, and it is easily adapted for a J-resolved representation that allows the use of a more reduced spectral width in the carbon dimension, obtaining higher levels of resolution within the same experimental time. We have also shown that small $^1D(CH)$ and $^2D(HH)$ RDCs can be measured for small molecules weakly aligned in anisotropic media. The proposed techniques are appropriate for routine use because require minimum set-up and afford simple data analysis and interpretation.

## 3. Methods and materials

The isotropic samples used in this work were 0.12 M strychnine dissolved in $CDCl_3$ (**1**), 0.14 M 5-methylene-2-norbornene dissolved in $CDCl_3$ (**2**) and 0.13 M progesterone dissolved in DMSO (**3**) (see chemical structures in Scheme 1). For the measurement of RDCs, 10 mg of **2** was aligned in a poly(methyl methacrylate) (PMMA) gel swollen in $CDCl_3$ using the reversible compression/relaxation method [40]. The $^2$H quadrupolar splitting ($\Delta\nu Q$) for the $CDCl_3$ signal was of 24 Hz. NMR experiments on **1** and **3** were recorded on a BRUKER DRX-500 spectrometer equipped with a 3-channel 5-mm cryoprobe incorporating a z-gradient coil. NMR experiments on **2** were carried out in a Bruker Avance 600 spectrometer equipped with a TXI HCN z-grad probe. The temperature for all measurements was set to 298 K.

In all experiments, the inter-pulse $\Delta$ (=$1/(2*{}^1J(CH))$ delays were set to 3.5 ms (optimized to $^1J(CH)$=145 Hz). Gradient ratios for G1:G2:G3 were set to 80:20.1:13, measured as percentage of the absolute gradient strength of 53.5 G/cm. Sine bell shaped gradients of 1 ms of duration and followed by a recovery delay of 100 μs were used. $^1$H saturation during the entire pre-scan delay was accomplished applying a 2.5 kHz WALTZ-16 modulated pulse train. Broadband $^{13}$C decoupling during acquisition was achieved applying a 8 kHz GARP modulated pulse train. All experiments were acquired and processed using the echo/anti-echo protocol where the gradient G1 was inverted for every second FID. An scaling factor $k = 8$ were used for the correlation experiments for all compounds. The J-resolved spectra were acquired omitting the $t_{1/2} - 180(^1H) - t_{1/2}$ element in the pulse sequence of Fig. 1 and reducing the spectral width in the indirect $\omega_1$ dimension to 500 Hz.

For spectra of Figs. 3, 2 scans were accumulated for each one of the 256 $t_1$ increments and the number of data points in $t_2$ was set to 2048. The recycle delay was set to 1 s for $\omega_1$-HSQC type experiments (Fig. 3A and C) and 3 s for $\omega_1$-iINEPT type experiments (Fig. 3B and D). Spectra 3A and 3B were acquired with an spectral window of 5000 Hz (in $\omega_2$) and 20,000 Hz (in $\omega_1$) giving a FID resolution of 2.4 and 9.8 Hz, respectively. Prior to Fourier-transformation of each data, zero filling to 4096 in $\omega_2$, 1024 in $\omega_1$ and a $\pi/2$-shifted sine-squared window function in both dimensions were applied. After applying zero filling the digital resolution was 1.2 and 2.4 Hz, respectively. In spectra of Figs. 3C and 3D, the spectral window in $\omega_1$ dimension was reduced to 500 Hz giving a FID resolution of 2.4 Hz (in $\omega_2$) and 1.9 Hz (in $\omega_1$). After applying zero filling the digital resolution was 1.2 and 0.5 Hz, respectively.

In the $\omega_1$-iINEPT-J experiments recorded on **2** in isotropic and anisotropic media (Fig. 5), a recycle delay of 3 s was used, 4 scans were accumulated for each one of the 256 $t_1$ increments and the number of data points in $t_2$ was set to 2048. Both of them were acquired with an spectral window of 3600 Hz (in $\omega_2$) and 500 Hz (in $\omega_1$) giving a FID resolution of 1.8 and 1.9 Hz, respectively. Prior to Fourier-transformation of each data, zero filling to 4096 in $\omega_2$, 1024 in $\omega_1$ and a $\pi/2$-shifted sine-squared window function in both dimensions were applied. After applying zero filling the digital resolution was 0.9 and 0.5 Hz, respectively. In the $\omega_1$-iINEPT experiment recorded on **3** (Fig. 6), a recycle delay of 3 s was used, 4 scans were recorded for each one of the 256 $t_1$ increments and the number of data points in $t_2$ was set to 2048 in all the experiments. Data were acquired with an spectral window of 2000 Hz (in $\omega_2$) and 12,500 Hz (in $\omega_1$) giving a FID resolution of 1.0 and 6.1 Hz, respectively. Prior to Fourier-transformation of each data, zero filling to 4096 in $\omega_2$, 1024 in $\omega_1$ and a $\pi/2$-shifted sine-squared window function in both dimensions were applied. After applying zero filling the digital resolution was 0.5 and 1.5 Hz, respectively.

## Acknowledgments

Financial support for this research provided by MINECO (project CTQ2012-32436) is gratefully acknowledged. Authors thanks to R.R. Gil and A. Navarro-Vázquez for a sample of PMMA gel. We also thank the Servei de Ressonància Magnètica Nuclear, Universitat Autònoma de Barcelona, for allocating instrument time to this project.

## Appendix A. Supplementary material

Supplementary data associated with this article can be found, in the online version, at http://dx.doi.org/10.1016/j.jmr.2014.02.003.

## References

[1] C.M. Thiele, Residual dipolar couplings (RDCs) in organic structure determination, Eur. J. Org. Chem. (2008) 5673–5685.
[2] G. Kummerlowe, B. Luy, Residual dipolar couplings for the configurational and conformational analysis of organic molecules, Annu. Rep. NMR Spectrosc. 68 (2009) 193–230.
[3] G. Kummerlowe, B. Luy, Residual dipolar couplings as a tool in determining the structure of organic molecules, Trend Anal. Chem. 28 (2009) 483–493.
[4] A. Enthart, J.C. Freudenberger, J. Furrer, H. Kessler, B. Luy, The CLIP/CLAP HSQC: pure absorptive spectra for the measurement of one-bond couplings, J. Magn. Reson. 192 (2008) 314–322.
[5] C.M. Thiele, Simultaneous assignment of all diastereotopic protons in strychnine using RDCs: PELG as alignment medium for organic molecules, J. Org. Chem. 69 (2004) 7403–7413.
[6] B.W. Yu, H. van Ingen, S. Vivekanandan, C. Rademacher, S.E. Norris, D.I. Freedberg, More accurate $^1$JCH coupling measurement in the presence of $^3$JHH strong coupling in natural abundance, J. Magn. Reson. 215 (2012) 10–22.
[7] B.W. Yu, H. van Ingen, D.I. Freedberg, Constant time INEPT CT-HSQC (CTi-CT-HSQC) – a new NMR method to measure accurate one-bond J and RDCs with strong 1H–1H couplings in natural abundance, J. Magn. Reson. 228 (2013) 159–165.
[8] P. Tzvetkova, S. Simova, B. Luy, P.E. HSQC: a simple experiment for the simultaneous and sign-sensitive measurement of ($^1$JCH + DCH) and ($^2$JHH + DHH) couplings, J. Magn. Reson. 186 (2007) 193–200.
[9] K. Fehér, S. Berger, K.E. Kövér, Accurate determination of small one-bond heteronuclear residual dipolar couplings by F1 coupled HSQC modified with a G-BIRD(r) module, J. Magn. Reson. 163 (2003) 340–346.
[10] C.M. Thiele, W. Bermel, Speeding up the measurement of one-bond scalar (1J) and residual dipolar couplings (1D) by using non-uniform sampling (NUS), J. Magn. Reson. 216 (2012) 134–143.
[11] K.E. Kövér, K. Fehér, Measurement of one-bond heteronuclear dipolar coupling contributions for amine and diastereotopic protons, J. Magn. Reson. 168 (2004) 307–313.
[12] L. Ziani, J. Courtieu, D. Merlet, Visualisation of enantiomers via insertion of a BIRD module in X-H correlation experiments in chiral liquid crystal solvent, J. Magn. Reson. 183 (2006) 60–67.
[13] U.R. Prabhu, S.R. Chaudhari, N. Suryaprakash, Visualization of enantiomers and determination of homo- and hetero-nuclear residual dipolar and scalar couplings: the natural abundant $^{13}$C edited J/D-resolved NMR techniques, Chem. Phys. Lett. (2010) 334–341.
[14] J. Furrer, M. John, H. Kessler, B. Luy, J-spectroscopy in the presence of residual dipolar couplings: determination of one-bond coupling constants and scalable resolution, J. Biomol. NMR 37 (2007) 231–243.
[15] M. Ottiger, F. Delaglio, J.L. Marquardt, N. Tjandra, A. Bax, Measurement of Dipolar Couplings for methylene and methyl sites in weakly oriented macromolecules and their use in structure determination, J. Magn. Reson. 124 (1998) 365–369.
[16] T.N. Pham, T. Liptaj, K. Bromek, D. Uhrín, Measurement of small one-bond proton-carbon residual dipolar coupling constants in partially oriented $^{13}$C natural abundance oligosaccharide samples. Analysis of heteronuclear $^1$JCH-modulated spectra with the BIRD inversion pulse, J. Magn. Reson. 157 (2002) 200–209.
[17] T. Carlomagno, W. Peti, C. Griesinger, A new method for the simultaneous measurement of magnitude and sign of $^1$DCH and $^1$DHH dipolar couplings in methylene groups, J. Biomol. NMR 17 (2000) 99–109.
[18] P. Permi, A spin-state-selective experiment for measuring heteronuclear one-bond and homonuclear two-bond couplings from an HSQC-type spectrum, J. Biomol. NMR 22 (2002) 27–35.
[19] E. Miclet, D.C. Williams Jr., G.M. Clore, D.L. Bryce, J. Boisbouvier, A. Bax, Relaxation-optimized NMR spectroscopy of methylene groups in proteins and nucleic acids, J. Am. Chem. Soc. 126 (2004) 10560–10570.
[20] G. Guichard, A. Violette, G. Chassaing, E. Miclet, Solution structure determination of oligoureas using methylene spin state selective NMR at $^{13}$C natural abundance, Magn. Reson. Chem. 46 (2008) 918–924.

[21] T. Parella, M. Gairí, Simultaneous recording of spin-state-selective NMR spectra for different $I_nS$ spin systems, J. Am. Chem. Soc. 126 (2004) 9821–9826.
[22] P. Permi, Two simple NMR experiments for measuring dipolar couplings in asparagine and glutamine side chains, J. Magn. Reson. 153 (2001) 267–272.
[23] E. Miclet, E. O'Neil-Cabello, E.P. Nikonowicz, D. Live, A. Bax, $^1$H–$^1$H dipolar couplings provide a unique probe of RNA backbone structure, J. Am. Chem. Soc. 125 (2003) 15740–15741.
[24] P. Nolis, J.F. Espinosa, T. Parella, Optimum spin-state-selection for all multiplicities in the acquisition dimension of the HSQC experiment, J. Magn. Reson. 180 (2006) 39–50.
[25] P. Nolis, T. Parella, Solution-state NMR experiments based on heteronuclear cross-polarization, Curr. Anal. Chem. 3 (2007) 47–68.
[26] M. Liu, R.D. Farrant, J.M. Gillam, J.K. Nicholson, J.C. Lindon, Selective inverse-detected long-range heteronuclear *J*-resolved NMR spectroscopy and its application to the measurement of $^3$JCH, J. Magn. Reson. B 109 (1995) 275–283.
[27] K. Kobzar, H. Kessler, B. Luy, Stretched gelatin gels as chiral alignment media for the discrimination of enantiomers by NMR spectroscopy, Angew. Chem. Int. Ed. 44 (2005) 3145–3147.
[28] J. Saurí, L. Castañar, P. Nolis, A. Virgili, T. Parella, P.E. HSQMBC: simultaneous measurement of proton–proton and proton–carbon coupling constants, J. Magn. Reson. 224 (2012) 101–106.
[29] J.R. Garbow, D.P. Weitekamp, A. Pines, Bilinear rotation decoupling of homonuclear scalar interactions, Chem. Phys. Lett. 93 (1982) 504–509.
[30] D. Uhrín, T. Liptaj, K.E. Kövér, Modified BIRD pulses and design of heteronuclear pulse sequences, J. Magn. Reson. A 101 (1993) 41–46.
[31] C. Griesinger, O.W. Sørensen, R.R. Ernst, Two-dimensional correlation of connected NMR transitions, J. Am. Chem. Soc. 107 (1985) 6394–6396.
[32] L. Mueller, P.E-COSY, a simple alternative to E.COSY, J. Magn. Reson. 72 (1986) 191–196.
[33] C. Griesinger, O.W. Sørensen, R.R. Ernst, Practical aspects of the E.COSY technique. Measurement of scalar spin-spin coupling constants in peptides, J. Magn. Reson. 75 (1987) 474–492.
[34] Y. Takayama, D. Sahu, J. Iwahara, Observing in-phase single-quantum $^{15}$N multiplets for $NH_2$/$NH_3^+$ groups with two-dimensional heteronuclear correlation spectroscopy, J. Magn. Reson. 194 (2008) 313–316.
[35] W.P. Aue, L. Muller, R.R. Ernst, Phase separation in two-dimensional spectroscopy, J. Magn. Reson. 28 (1977) 29–39.
[36] B. Luy, K. Kobzar, H. Kessler, An easy and scalable method for the partial alignment of organic molecules for measuring residual dipolar couplings, Angew. Chem. Int. Ed. 43 (2004) 1092–1094.
[37] A. Bagno, F. Rastrelli, G. Saielli, Toward the complete prediction of the $^1$H and $^{13}$C NMR spectra of complex organic molecules by DFT methods: application to natural substances, Chem. Eur. J. 12 (2006) 5514–5525.
[38] M. Misiak, W. Koźmiński, Determination of heteronuclear coupling constants from 3D HSQC-TOCSY experiment with optimized random sampling of evolution time space, Magn. Reson. Chem. 47 (2009) 205–209.
[39] J.C. Cobas, V. Constantino-Castillo, M. Martín-Pastor, F. del Río Portilla, A two-stage approach to automatic determination of 1H NMR coupling constants, Magn. Reson. Chem. 43 (2005) 843–848.
[40] C. Gayathri, N.V. Tsarevsky, R.R. Gil, RDCs analysis of small molecules made easy: fast and tuneable alignment by reversible compression/relaxation of reusable PMMA gels, Chem. Eur. J. 16 (2010) 3622–3626.
[41] G. Kontaxis, A. Bax, Multiplet component separation for measurement of methyl $^{13}$C–$^1$H dipolar couplings in weakly aligned proteins, J. Biomol. NMR 20 (2001) 77–82.